Lecture 1: Neutral brushes. Scaling model of a neutral planar polymer brush (mushroom and brush regimes). Effect of solvent. Strong stretching approximation: chain trajectory and parabolic potential. Internal structure of a planar brush. Response of polymer brush to compression. Curved polymer brushes. Scaling model of star-like and comb-like molecular brushes (stars and combs in solution).

Lecture 2: Charged brushes. Strong and weak polyelectrolytes. Scaling model of strong PE planar brush. Main regimes of PE brush (counterion and salt dominated). Local electroneutrality approximation. Parabolic potential and internal structure of planar PE brush. Interactions between planar PE brushes. Curved PE brushes (scaling model).
Corona of neurofilament (NF) as a cylindrical PE brush.

Lecture 3: Polymer micelles.

Micellization of neutral diblock copolymers in dilute solution in selective solvent. CMC. Strong segregation limit and narrow interface approximation. Starlike and crew-cut spherical micelles. Cylindrical and lamellar aggregates. Morphological transitions sphere-cylinder-lamella. Micelles with charged coronae.
Diblock copolymer aggregates in semi-dilute solutions and melts. Strong and weak segregation limits.
Multi-compartment micelles (MCMs).

Micellization of diblock copolymer in selective solvent

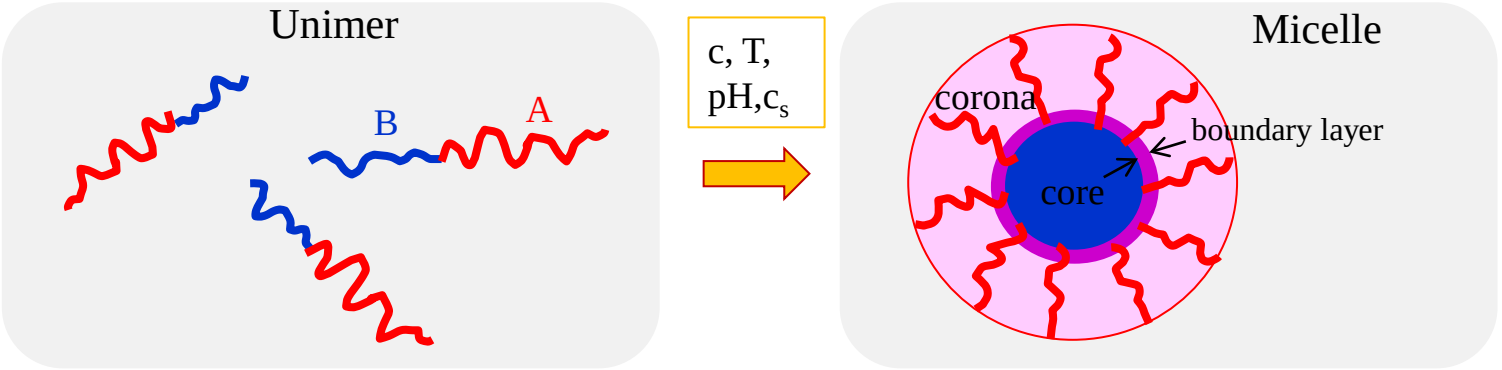

Static light scattering measurements $Kc/R_\theta = 1/M_w + 2A_2c + \ldots$

Dynamic light scattering measurements Stokes–Einstein equation, $D = kT/6\pi\eta R_h$

X-ray diffraction experiments size distribution of micelles

Sample morphology

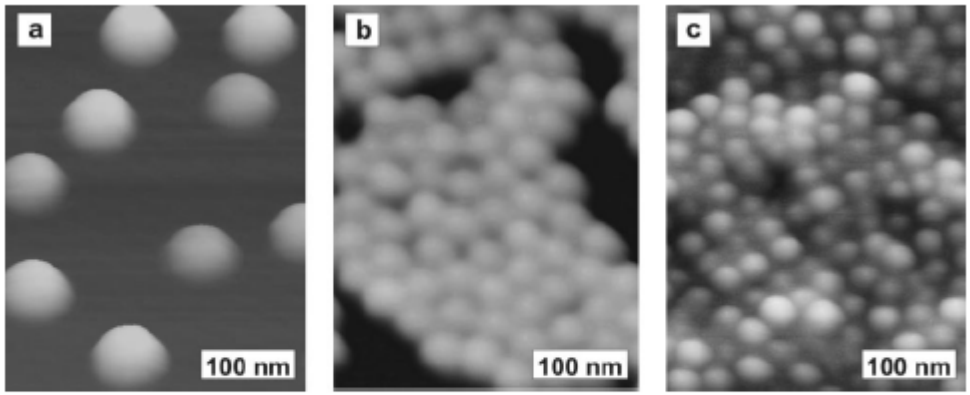

Figure 1. AFM height images of PS-*b*-PI spherical micelles formed from (a) sample 39−94 (R_h = 54 nm), (b) sample 39−15 (R_h = 32 nm), and (c) sample 19−14 (R_h = 20 nm). The micelles reduce in size upon decreasing the length of the soluble polyisoprene (PI) block (a, b) as well as the length of the insoluble polystyrene (PS) block (b, c).

Nomenclature

Star-like micelle: H >> R; R_{total}= H

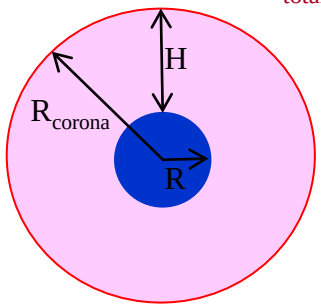

Crew-cut micelle: H << R; R_{total}= R

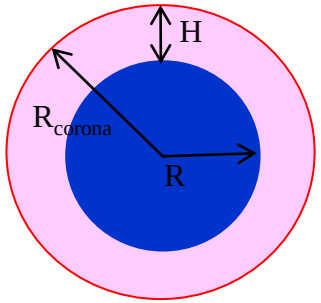

Critical micelle concentration (CMC)

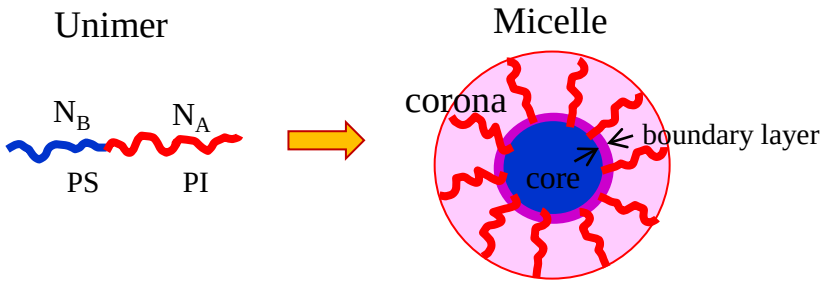

La Rue et al, 2008

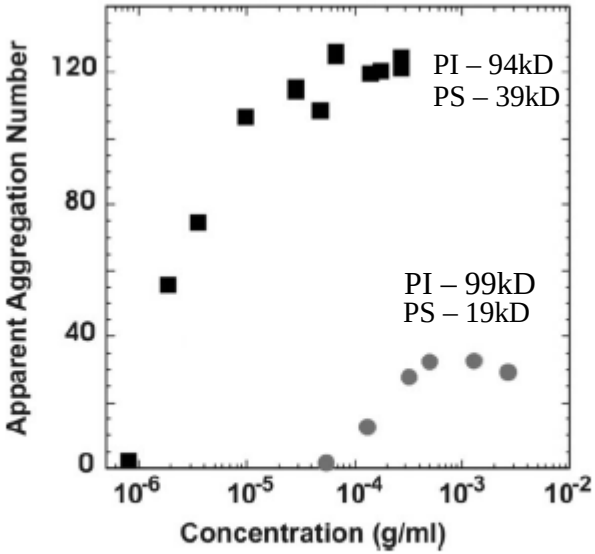

Figure 2. Plot of the apparent aggregation number vs concentration for PS-*b*-PI 39-94 (black squares) and 19-99 (gray circles) measured at 25 °C in *n*-heptane.

La Rue et al, 2008

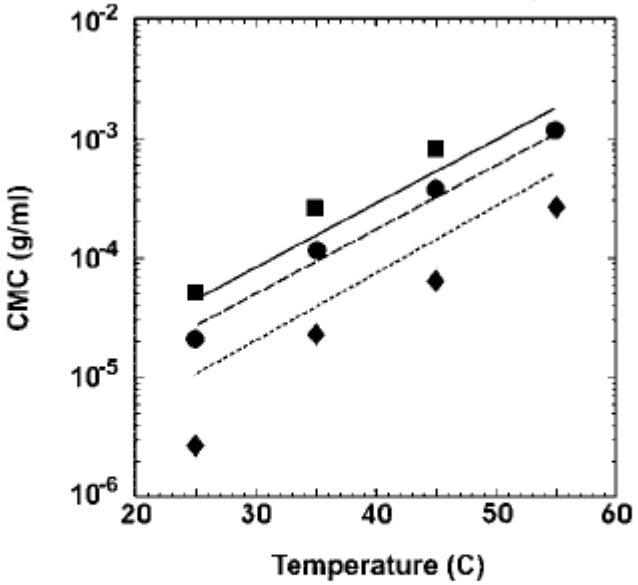

Figure 3. Plot of the variation of the CMC with temperature for samples 19-26 (diamonds), 19-59 (circles), and 19-99 (squares). Theoretical calculations for PI blocks with molecular weights of 26, 59, and 99 kDa are shown respectively by the dotted, dashed, and solid lines.

Critical micelle concentration (theory)

(V, N_p, T) total number density of the amphiphiles is $c = N_p/V$

c_1 is the concentration (number density) of unimer

$c_{\text{mic}} = (c - c_1)/p$ concentration of the monodisperse micelles with aggregation number p

Helmholtz free energy

$$F/Vk_BT = pc_{\text{mic}}F_p/k_BT + c_{\text{mic}}(\ln c_{\text{mic}} - 1) + c_1F_1/k_BT + c_1(\ln c_1 - 1)$$

↑ free energy per molecule in micelle with aggregation number p

The minimization ($\partial F/\partial p = 0$, $\partial F/\partial c_{\text{mic}} = 0$) leads to the following equations:

$$p\frac{\partial F_p}{\partial p} = \frac{k_BT}{p}\ln c_{\text{mic}}$$

$$F_p + p\frac{\partial F_p}{\partial p} \equiv \frac{\partial (pF_p)}{\partial p} = \mu_1(c_1)$$

$\mu_1(c_1) = F_1 + k_BT\ln c_1$ is the chemical potential of unimer.

Often, the critical micelle concentration (CMC) is defined as the total concentration of amphiphiles at which the number of unimers is equal to the number of amphiphiles incorporated into the micelles, $pc_{\text{mic}} = c_1 = \text{CMC}/2$. In this case, the CMC is specified by the equation:

$$k_BT\ln\left(\frac{\text{CMC}}{2}\right) = \left(\frac{\partial (pF_p)}{\partial p}\right)_{p=p_{\text{eq}}(\text{CMC})} - F_1$$

where F_p is the free energy per chain in the equilibrium micelle with $p = p_{\text{eq}}(\text{CMC})$.

Critical micelle concentration (theory cont'd)

A frequently used simplifying approximation is based on neglecting the translational entropy of micelles

$$F/Vk_BT = pc_{mic}F_p/k_BT + c_{mic}(\ln c_{mic} - 1) + c_1F_1/k_BT + c_1(\ln c_1 - 1)$$

"Practical" equations:

$$\frac{\partial F_p(p)}{\partial p} = 0$$

Aggregation number p_0 in equilibrium micelle (does not depend on concentration of amphiphiles c)

$$c_1 = \exp\left[(F_p(p_0) - F_1)/k_BT\right]$$

Concentraton c_1 of unimers

$$c_{mic} = \frac{c - c_1}{p_0}$$

Concentraton c_{mic} of micelles

approximate expression for the CMC

$$k_BT \ln\left(\frac{\text{CMC}}{2}\right)_{\text{approx}} = F_p(p_0) - F_1$$

in order to find the optimal (equilibrium) aggregation number and the CMC, a theoretical model has to specify the functional form of the free energy F_p per amphiphile as a function of p in an aggregate of a given morphology.

Scaling model of spherical block copolymer micelle

Zhulina & Birshtein 1985; Halperin 1987

The free energy F_p per one block copolymer in a micelle can be presented as

$$F_p = F_{corona} + F_{interface} + F_{core}.$$

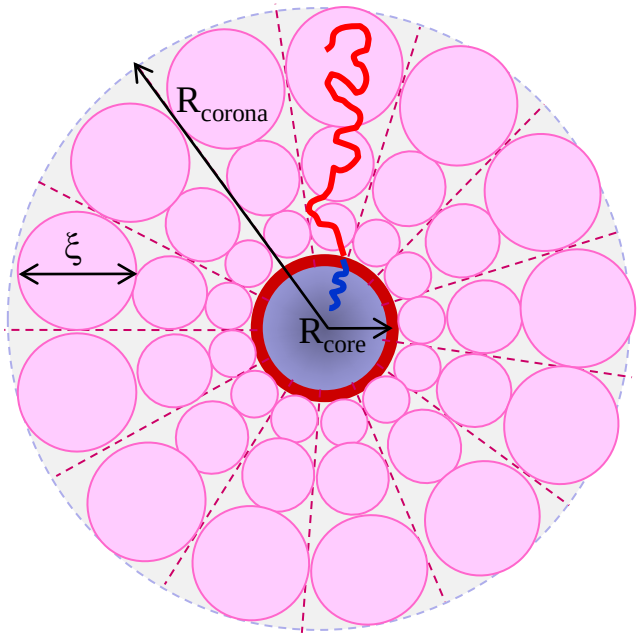

Core

$$R_{core} \cong (pN_B/\varphi)^{1/3}$$

φ – volume fraction of B in the core

$$F_{core}(p)/k_BT \cong R_{core}^2/N_B$$

Interface

$$s \cong R_{core}^2/p \cong (N_B/\varphi)^{2/3} p^{-1/3}$$

$$F_{interface}(p)/k_BT \cong \gamma s \cong \gamma \left(\frac{N_B}{\varphi}\right)^{2/3} p^{-1/3}$$

γ – surface tension

Corona (spherical brush)

$$\xi(r) \cong r/p^{1/2}$$

$$F_{corona}(p)/k_BT \cong p^{1/2} \ln\left(\frac{R_{corona}}{R_{core}}\right)$$

→ Star-like, $R_{corona} >> R_{core}$

→ Crew-cut, $R_{corona} << R_{core}$

Minimization of F_p with respect to p gives equilibrium aggregation number p_0

Important note: in stable spherical micelles F_{corona} ❒ $F_{interface} >> F_{core}$

Star-like spherical block copolymer micelle ($R_{corona} >> R_{core}$)

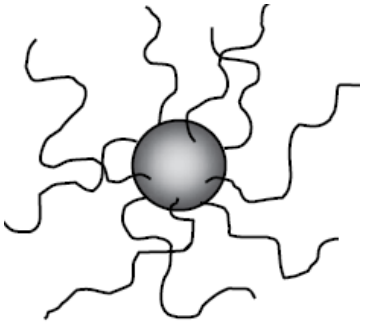

$$R_{corona} \cong N_A^{\nu} p^{(1-\nu)/2}$$ ($\nu \approx 3/5$ and $\nu = 1/2$ under good and theta-solvent conditions, respectively).

Equilibrium aggregation number

$$p_0 \cong \gamma^{6/5} (N_B/\varphi)^{4/5} \left(\ln \frac{R_{corona}}{R_{core}} \right)^{-6/5}$$

With the accuracy of the logarithmic factors,

$$R_{corona} \cong N_A^{\nu} v_A^{2\nu-1} \gamma^{3(1-\nu)/5} \left(\frac{N_B}{\varphi} \right)^{2(1-\nu)/5}$$

$$R_{core} \cong \gamma^{2/5} \left(\frac{N_B}{\varphi} \right)^{3/5}$$

$$F_p(p_0)/k_BT = \gamma^{3/5} \left(\frac{N_B}{\varphi} \right)^{2/5} \left(\ln \frac{R_{corona}}{R_{core}} \right)^{2/5}$$

$$\ln \mathrm{CMC} \approx -\gamma \left(\frac{N_B}{\varphi} \right)^{2/3} + \gamma^{3/5} \left(\frac{N_B}{\varphi} \right)^{2/5} \left(\ln \frac{R_{corona}}{R_{core}} \right)^{2/5}$$

$-F_1$ $\qquad$ $F_p(p_0)$

La Rue et al, 2008

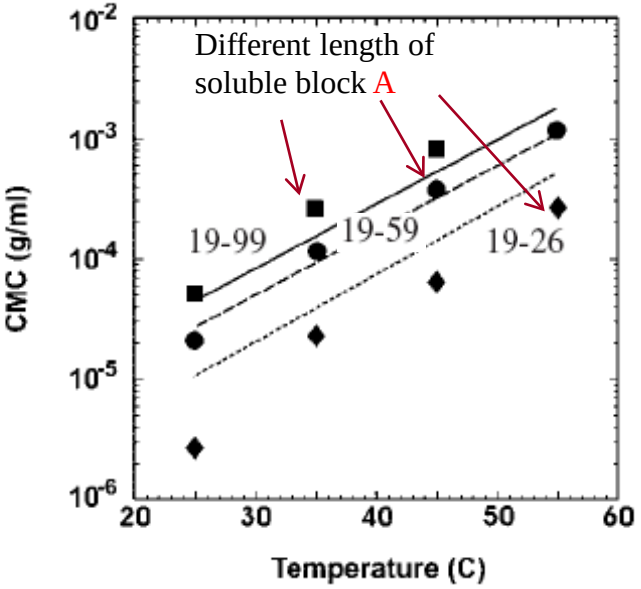

CMC depends most strongly on length of insoluble block B, but also on temperature T and length of soluble block A

Crew-cut spherical block copolymer micelle ($R_{corona} << R_{core}$)

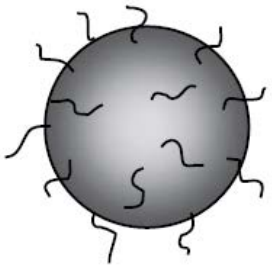

Corona is planar-like brush with $H_{corona} \cong N_A s^{-(1-\nu)/2\nu}$

$$F_{corona}/k_BT \cong H_{corona}/s^{1/2} \cong H_{corona}/\xi \cong N_A s^{-1/2\nu}$$

Dominant terms in the free energy per chain are the same for all morphologies of micelle (lamella, cylinder, sphere), $F_p/k_BT = \gamma s + N_A(s/a^2)^{-1/2\nu}$

Minimization with respect to s gives:

$$s_{eq} \cong \left(\frac{N_A}{\gamma}\right)^{2\nu/(2\nu+1)}$$

$$R_{core} \cong \frac{N_B}{\varphi}\left(\frac{N_A}{\gamma}\right)^{-2\nu/(2\nu+1)}$$

equilibrium aggregation number

$$p_0 \cong \left(\frac{N_B}{\varphi}\right)^2\left(\frac{N_A}{\gamma}\right)^{-6\nu/(2\nu+1)}$$

$$\ln \mathrm{CMC} \cong -\gamma(N_B/\varphi)^{2/3} + (\gamma N_A^{2\nu})^{1/(2\nu+1)}$$

La Rue et al, 2008

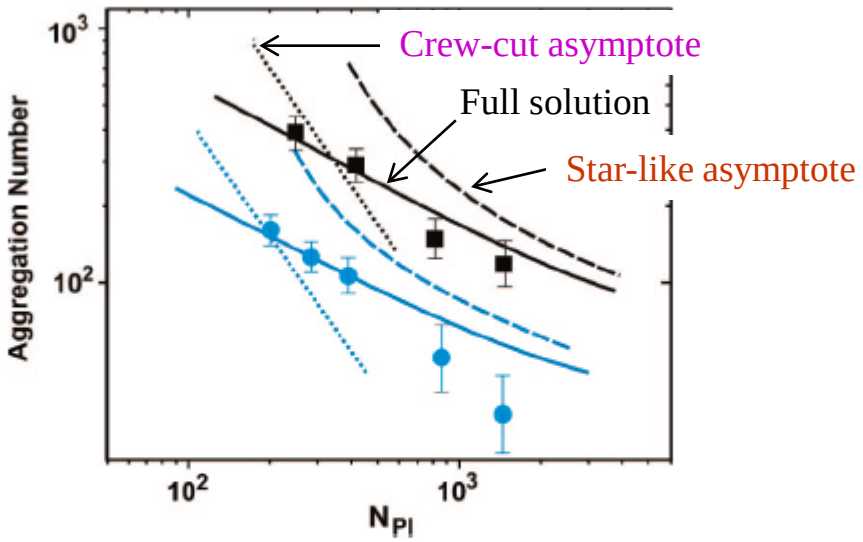

Figure 4. Log−log plots of the variation in the aggregation number with the degree of polymerization of the PI blocks. Black and blue symbols are for 39 and 19 kDa PS blocks respectively. The solid, dashed, and dotted lines are respectively the new crossover scaling solution, asymptotic star-like, and asymptotic crew-cut dependences.

Polymorphism in non-ionic micelles

In aggregates with $R_{corona} >> R_{core}$, spherical micelle is always most stable: at the same area per chain s, spherical corona has more space and is less extended due to intra-chain repulsions.

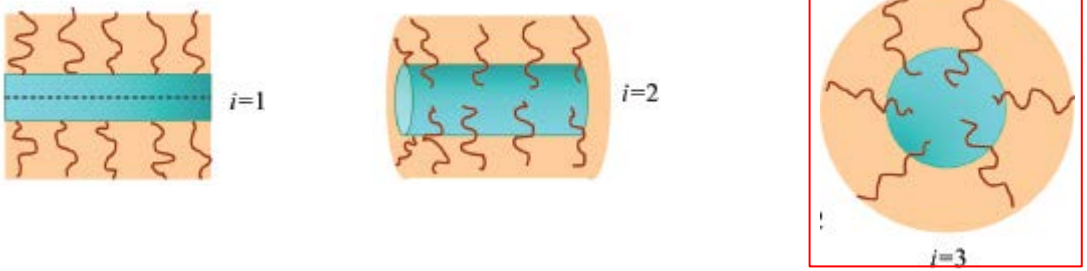

In crew-cut aggregates, dominant contributions to $F_p = F_{1(planar\ corona)} + \gamma s$ are the same for all *morphologies* *i=1,2,3*, but morphology-dependent corrections (ΔF_A and F_B) are different.

$$\frac{F_A}{k_B T} \approx \frac{F_1 + \Delta F_A}{k_B T} \simeq \frac{H_1}{\sqrt{s}} - \frac{(i-1)}{4\nu}\frac{H_1^2}{R\sqrt{s}}$$

F_{corona} ❒ F_A decreases in the row:lamella, cylinder, sphere

On the contrary, F_{core} increases in the row lamella, cylinder, sphere

$F_{core}/k_BT = b_i R_{core}^2/a^2 N_B$ with $b_1 = \pi^2/8$, $b_2 = \pi^2/16$ and $b_3 = 3\pi^2/80$ Semenov *JTEP* 1985

Balancing $\Delta F_A + F_{core}$ in morphologies, *i* and *(i+1)* we find binodals for morphological transitions *i* to *(i+1)*

Diagram of states

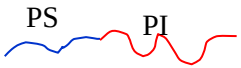

in n-heptane

Zhulina et al, 2005

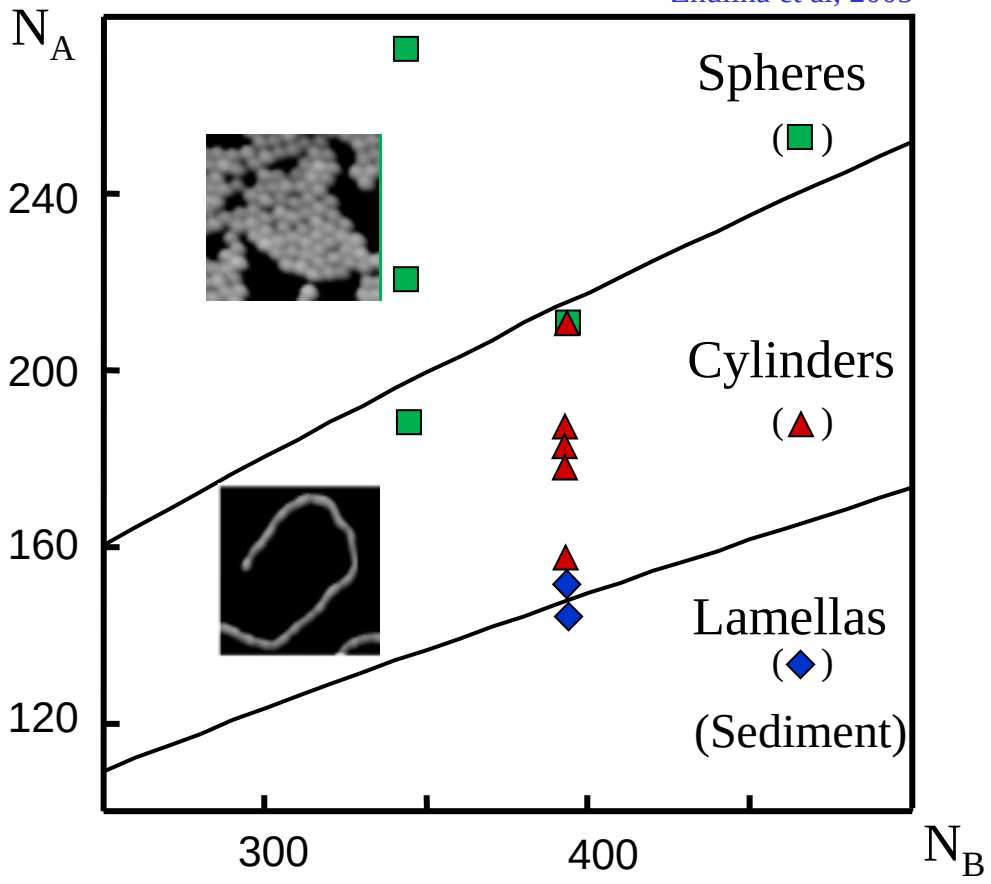

Micelles with charged corona

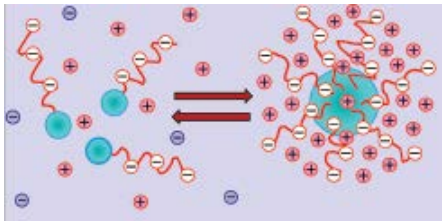

In experimentally relevant cases , coronal charge is compensated

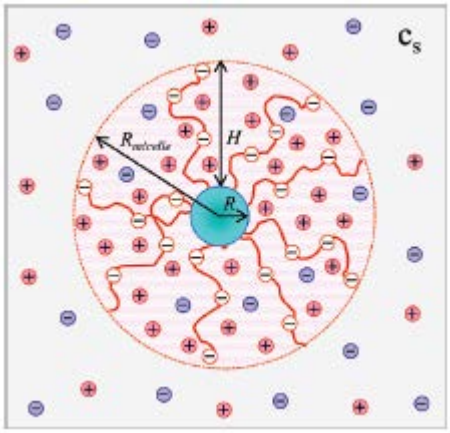

Low salt : $\alpha c >> c_s$

$$f_{ion}(r)/k_BT \approx \begin{cases} \alpha_b c_p(r)\{\ln[2\alpha_b c_p(r)/c_s] - 1\}, & \text{quenched PE} \\ c_p(r)[-\alpha(r) + \ln(1-\alpha(r))], & \text{annealing PE} \end{cases}$$

$$\alpha(r) \approx \begin{cases} \alpha_b, & \text{quenched PE} \\ \{\alpha_b c_s/[2(1-\alpha_b)c_p(r)]\}^{1/2}, & \text{annealing PE} \end{cases}$$

High salt : $\alpha c << c_s$

$$f_{ion}(r)/k_BT \approx \begin{cases} \alpha_b{}^2 c_p{}^2(r)/(2c_s), & \text{quenched PE} \\ \alpha_b{}^2 c_p{}^2(r)/(2c_s) + c_p(r)\ln(1-\alpha_b), & \text{annealing PE} \end{cases}$$

$$\alpha(r) \approx \alpha_b$$

$$\upsilon_{A,\text{eff}} = (\upsilon_A + \alpha_b{}^2/2c_s)$$

Novel micelle – to – micelle transition in annealing PEs

Xu et al 2007

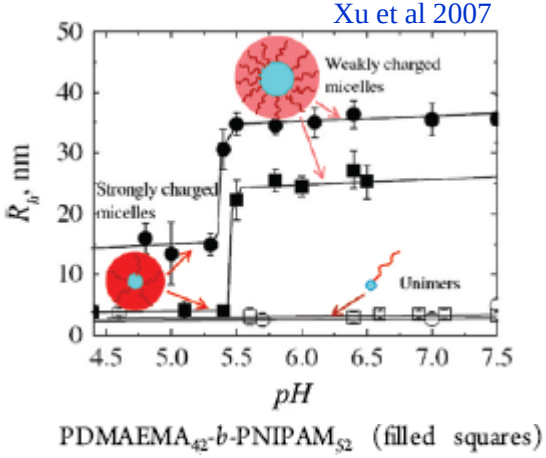

$PDMAEMA_{42}$-*b*-$PNIPAM_{52}$ (filled squares)

Morphological transitions . Same physics as in neutral aggregates

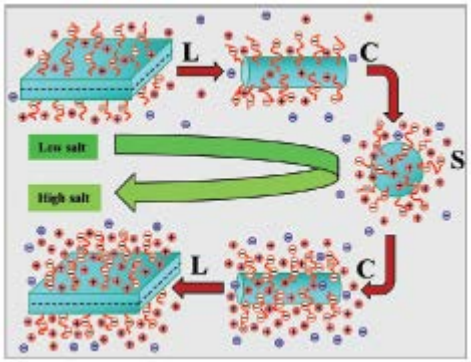

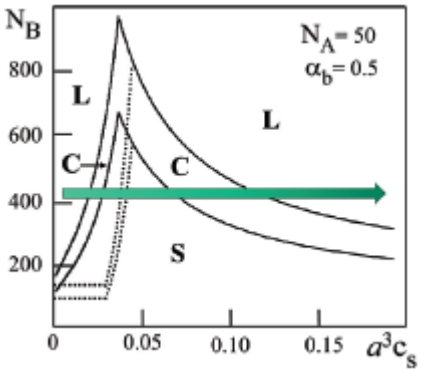

Dilute solution of neutral star-like micelles, $\varphi < \varphi^*$

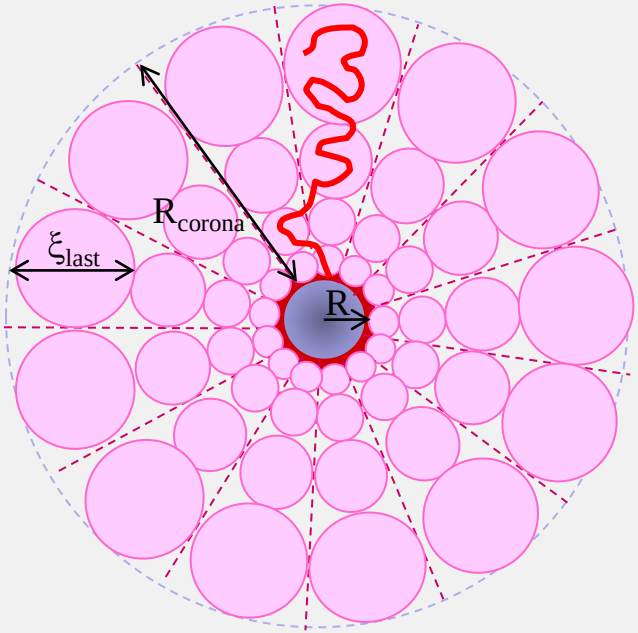

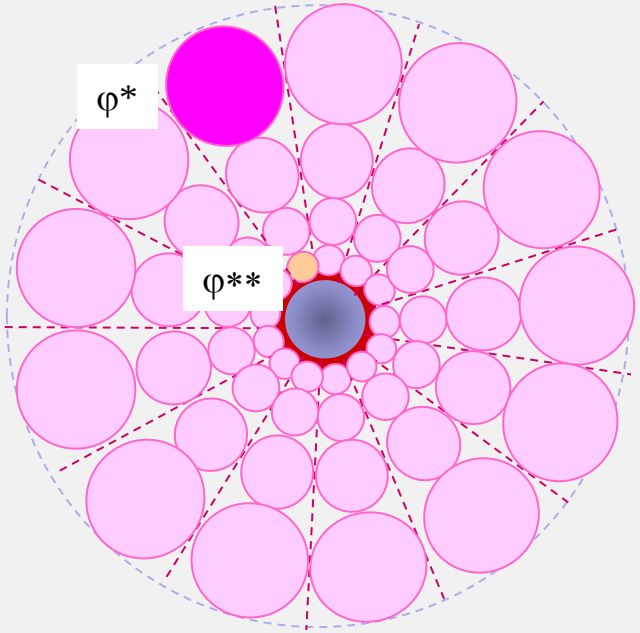

Semi-dilute solution of star-like micelles with $\varphi^* < \varphi < \varphi^{**}$

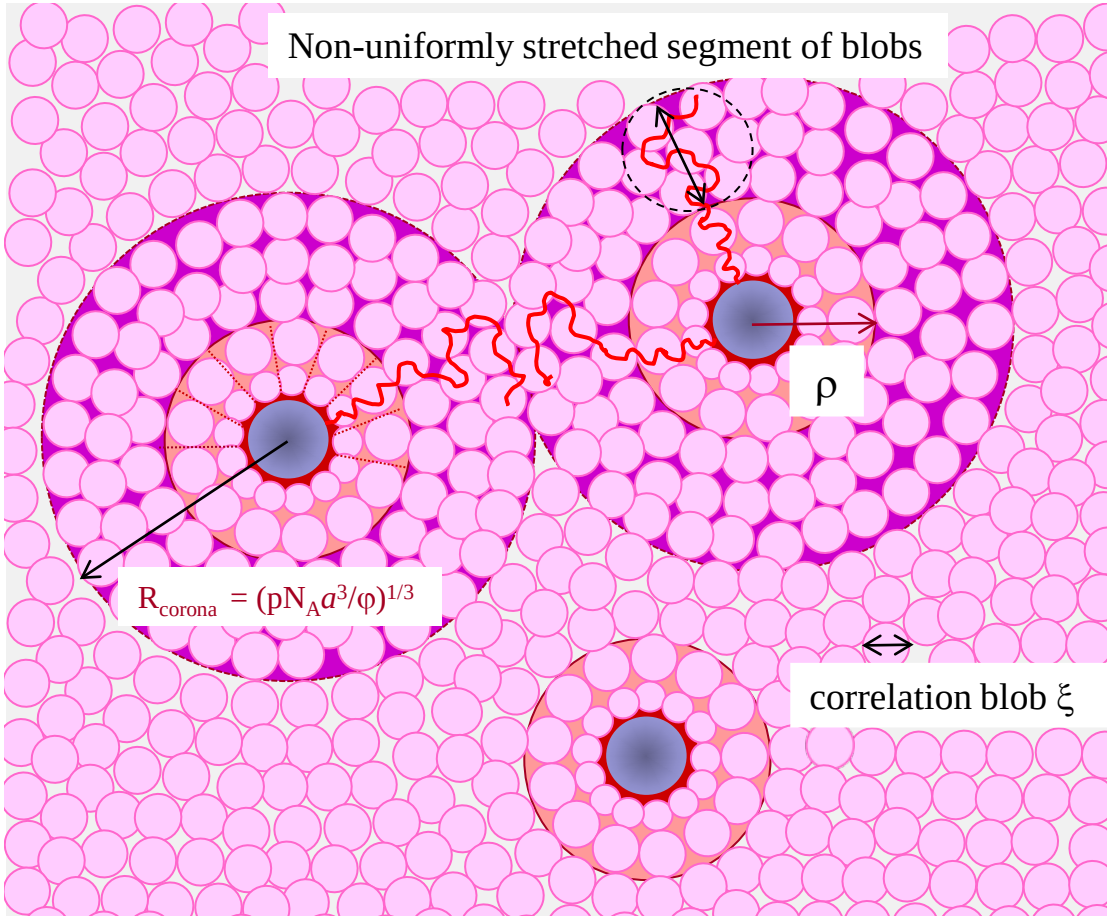

Micelles remain segregated (quasi-globular regime)

$$R_{corona} = (pN_A a^3/\varphi)^{1/3}$$

Aggregation number increases logarithmically with solution concentration

$$p = p_0 \ln((\varphi/\varphi^*)$$

Semi-dilute solution of star-like micelles with $\varphi > \varphi^{**}$

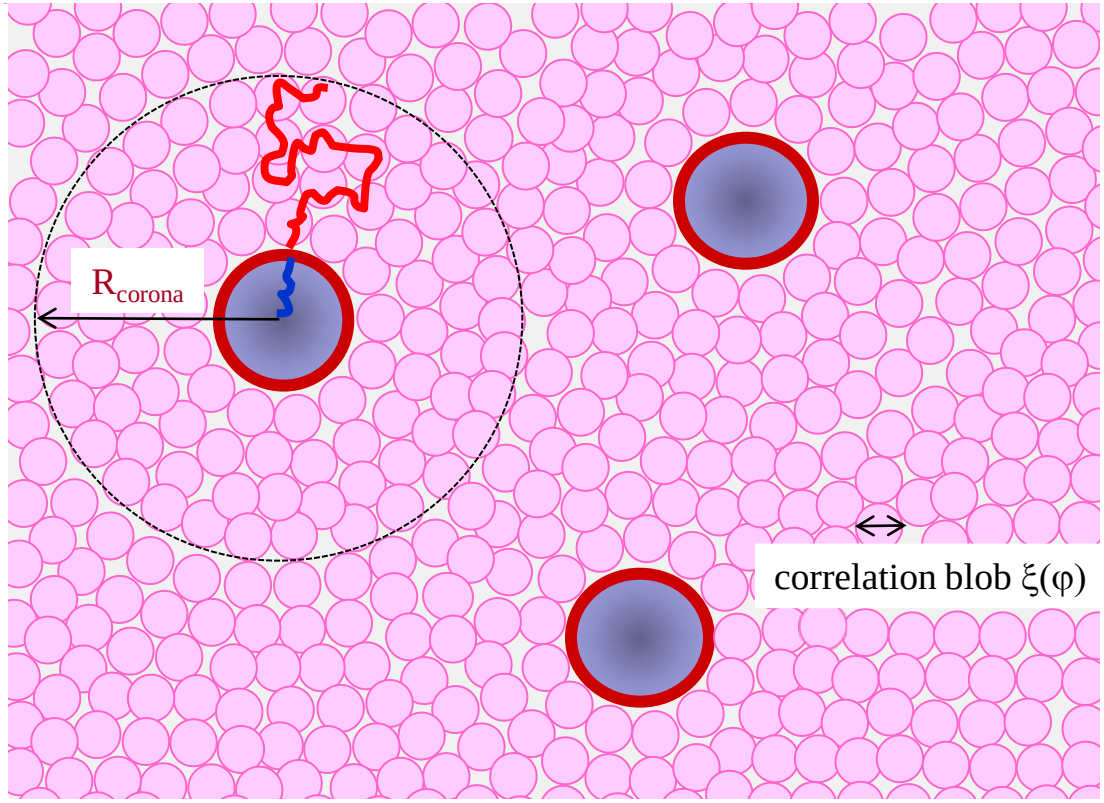

Micelles remain segregated (quasi-globular regime) due to retained stretching of coronal block, $R_{corona} = (pN_A a^3/\varphi)^{1/3}$

BUT aggregation number increases with solution concentration as

$$p = \gamma N_B \varphi^{3/4}$$

Diagram of states of concentrated solution of neutral block copolymer

Strong segregation limit (narrow interface, well defined domains)

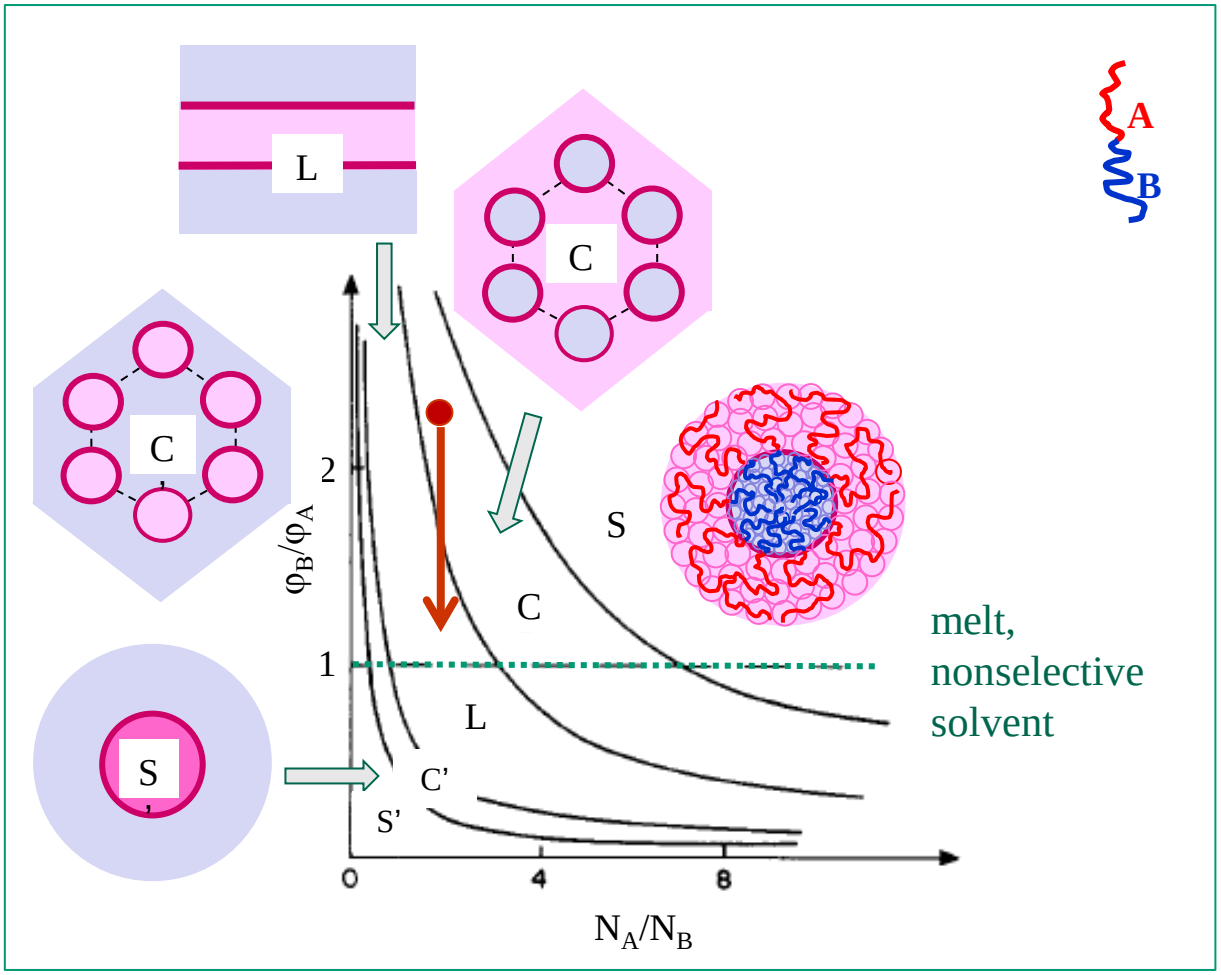

Transitions between morphologies are characterized by

$$s_{i+1} = s_i$$

$$R_{core,i+1} = R_{core,i}\ (i+1)/i$$

Polyisoprene – polymethylstyrene – polyisoprene (ABA) in decalin

Volkova et al 1982

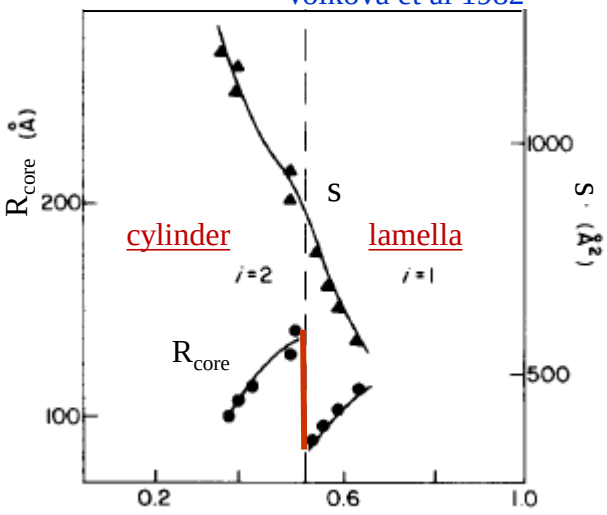

Polymer concentration $\varphi \sim \varphi_A$

Theoretical phase diagram of diblock copolymer melt

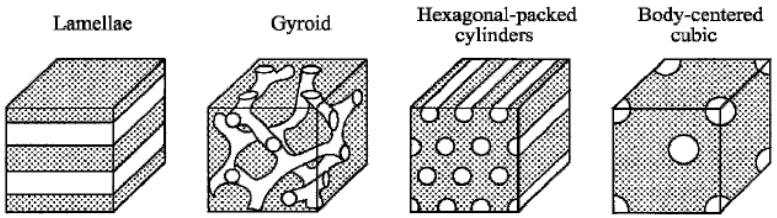

Leibler 1980, Semenov 1985, Fredrickson, Helfand 1987, Matsen 1996

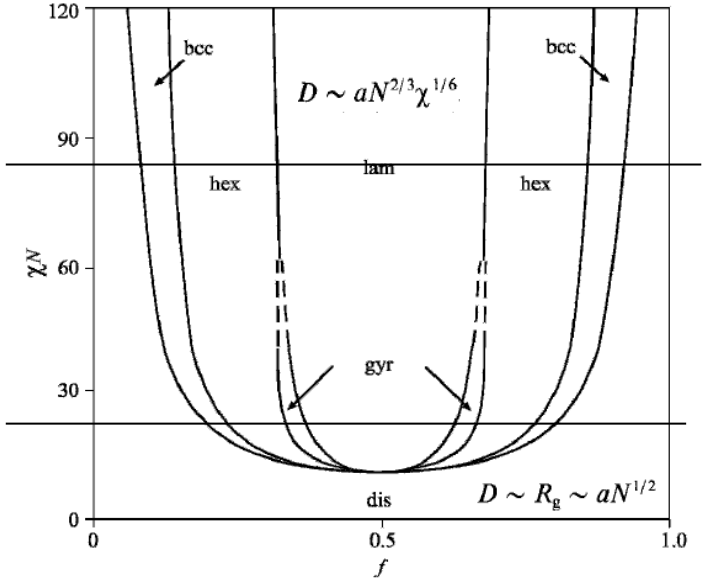

Strong segregation limit

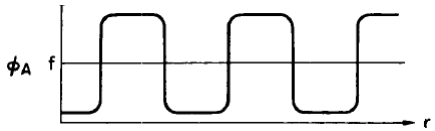

Intermediate range

Weak segregation limit

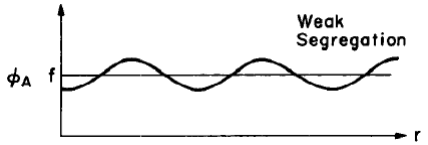

Figure 1.2 Phase diagram for a conformationally symmetric diblock copolymer, calculated using self-consistent mean field theory [49, 51], along with illustrations of the equilibrium morphologies. In the phase diagram, regions of stability of disordered (dis), lamellar (lam), gyroid (gyr), hexagonal (hex) and body-centred cubic (bcc) phases are indicated.

Recent advances: multi-compartment micelles (MCM) with well controlled morphology

Terpolymer ABC in selective solvent

PS-PB-PMMA

A B C

Step I: Dissolution of SBMs in DMAc (*N,N*-dimethylacetamide, non-solvent for PB,

Step II: dialysis against an acetone/isopropanol mixture

Acetone is a non-solvent for PB, a near-Θ solvent for PS and a good solvent for PMMA.
Isopropanol is a near-Θ solvent for PMMA and a non-solvent for both PS and PB

Groschel et al, Nature Communications 2012

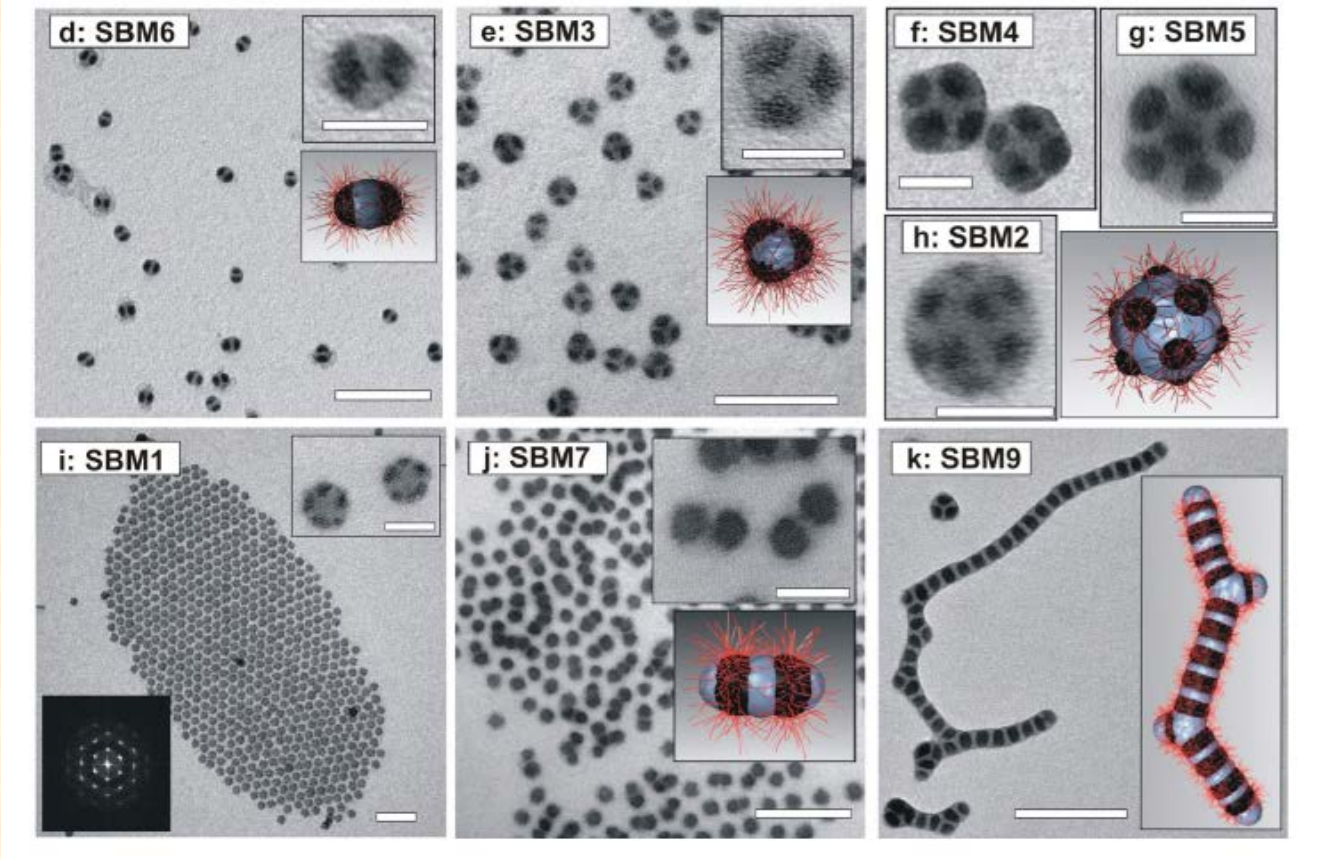

Recent advances: scaling model of MCM

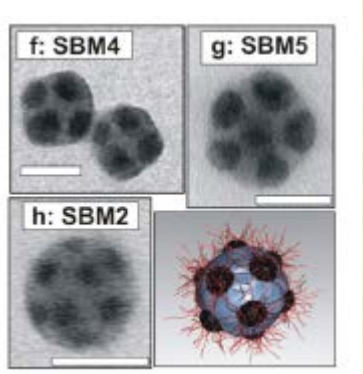

PS-PB-PMMA

A B C

$V_C = N_C a_C^3$

$V_B = N_B a_B^3$

$V_A = N_A a_A^3$

micelle comprises $p \gg 1$ chains

each B-domain (one patch) comprises $m = p/n$ chains

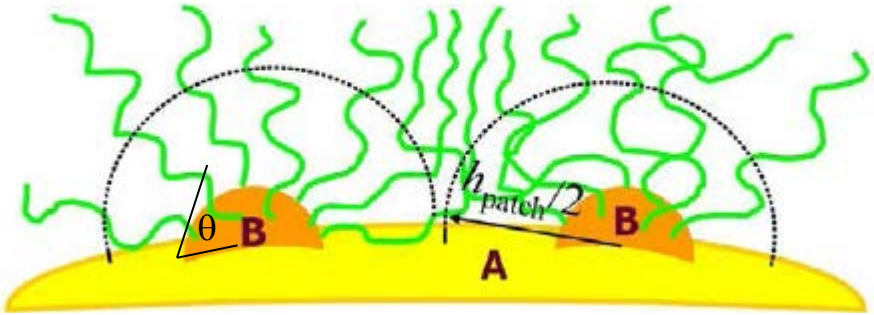

Schematic representation of a spherical MCM for the case $V_A >> V_B$

		V_A/V_B
SBM2	$S_{306}B_{151}M_{340}^{74}$	3.57
SBM4	$S_{660}B_{674}M_{350}^{140}$	1.72
SBM5	$S_{611}B_{635}M_{292}^{127}$	1.69

$$F = F_{corona} + \cancel{F_{core}} + F_{interface}$$

$$F_{interface} = F_{AS} + F_{BS} + F_{AB} = \gamma_{AS} S_{AS} + \gamma_{BS} S_{BS} + \gamma_{AB} S_{AB}$$

Conservation of material in B and A domains, ignore curvature of A domain,,etc

$V_A/V_B >> 1$

$$\frac{F_{interface}}{p} \simeq \tilde{\gamma}_{BS} m^{-1/3} V_B^{2/3} + \gamma_{AS} p^{-1/3} V_A^{2/3}$$

$$\tilde{\gamma}_{BS} \simeq \gamma_{BS} (1-\cos\theta)^{2/3} \left(1+\frac{\cos\theta}{2}\right)^{1/3}$$

modified surface tension at BS boundary

Star-like corona of MCM is split into n coronas around B-patches and peripheral (laterally uniform) part

$$\frac{F_{corona}}{p} = m^{1/2} \ln \frac{R_{core}}{R_B n^{1/2}} + p^{1/2} \ln \frac{R_{micelle}}{R_{core}(1+n^{-1/2})}$$

Minimization with respect to p and m: $p \cong (N_A v_A)^{4/5} \gamma_{AS}^{6/5} \ln^{-6/5}(R_{micelle}/R_{core})$ (like for diblock AC)

Number of patches $n \cong (N_A v_A / N_B v_B)^{4/5} (\gamma_{AS}/\tilde{\gamma}_{BS})^{6/5} \ln^{-6/5}(R_{micelle}/R_{core})$